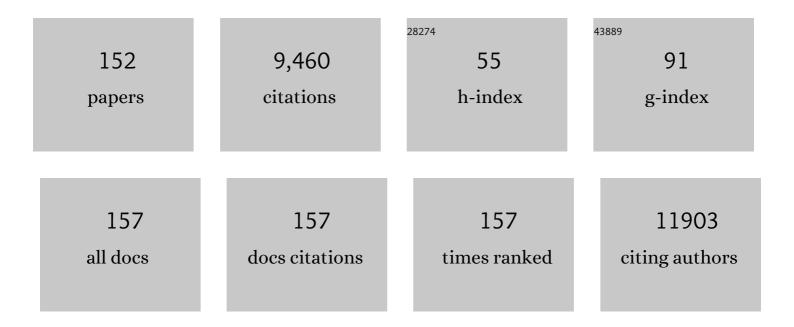
Yijun Zhong

List of Publications by Year in descending order

Source: https://exaly.com/author-pdf/7803862/publications.pdf Version: 2024-02-01



YUUN ZHONC

#	Article	IF	CITATIONS
1	Optimization strategies on the advanced engineering of Co-based nanomaterials for electrochemical oxygen evolution. Journal of Alloys and Compounds, 2022, 890, 161929.	5.5	12
2	Engineering hierarchical porous ternary Co-Mn-Cu-S nanodisk arrays for ultra-high-capacity hybrid supercapacitors. Journal of Colloid and Interface Science, 2022, 612, 298-307.	9.4	26
3	In-situ photodeposition of cadmium sulfide nanocrystals on manganese dioxide nanorods with rich oxygen vacancies for boosting water-to-oxygen photooxidation. Journal of Colloid and Interface Science, 2022, 613, 764-774.	9.4	19
4	Hierarchical mesoporous S,N-codoped carbon nanostructures composed of Co/Co-Cu-S/carbon nanoplate arrays on carbon nanofibers as a self-supported air cathode for long-lasting rechargeable Zn-air batteries. Science China Technological Sciences, 2022, 65, 693-703.	4.0	6
5	Defect engineering of electrode materials towards superior reaction kinetics for high-performance supercapacitors. Journal of Materials Chemistry A, 2022, 10, 15267-15296.	10.3	38
6	Molecule-assisted modulation of the high-valence Co3+ in 3D honeycomb-like CoxSy networks for high-performance solid-state asymmetric supercapacitors. Science China Materials, 2021, 64, 840-851.	6.3	55
7	New types of hybrid electrolytes for supercapacitors. Journal of Energy Chemistry, 2021, 57, 219-232.	12.9	106
8	Approach of fermi level and electron-trap level in cadmium sulfide nanorods via molybdenum doping with enhanced carrier separation for boosted photocatalytic hydrogen production. Journal of Colloid and Interface Science, 2021, 583, 661-671.	9.4	83
9	Fabrication of an Au ₂₅ â€Cysâ€Mo Electrocatalyst for Efficient Nitrogen Reduction to Ammonia under Ambient Conditions. Small, 2021, 17, e2100372.	10.0	30
10	Recent advances in the synthesis of non-carbon two-dimensional electrode materials for the aqueous electrolyte-based supercapacitors. Chinese Chemical Letters, 2021, 32, 3733-3752.	9.0	14
11	Synergistic effects of Fe and Mn dual-doping in Co3S4 ultrathin nanosheets for high-performance hybrid supercapacitors. Journal of Colloid and Interface Science, 2021, 590, 226-237.	9.4	46
12	Precise regulation of pyrroleâ€ŧype singleâ€atom Mnâ€N ₄ sites for superior pHâ€universal oxygen reduction. , 2021, 3, 856-865.		60
13	One-step phosphorization preparation of gradient-P-doped CdS/CoP hybrid nanorods having multiple channel charge separation for photocatalytic reduction of water. Journal of Colloid and Interface Science, 2021, 596, 431-441.	9.4	54
14	Oxygen-vacancy-assisted construction of FeOOH/CdS heterostructure as an efficient bifunctional photocatalyst for CO2 conversion and water oxidation. Applied Catalysis B: Environmental, 2021, 293, 120203.	20.2	71
15	pH-induced hydrothermal synthesis of Bi2WO6 nanoplates with controlled crystal facets for switching bifunctional photocatalytic water oxidation/reduction activity. Journal of Colloid and Interface Science, 2021, 602, 868-879.	9.4	27
16	Trifunctional electrocatalyst of N-doped graphitic carbon nanosheets encapsulated with CoFe alloy nanocrystals: The key roles of bimetal components and high-content graphitic-N. Applied Catalysis B: Environmental, 2021, 298, 120512.	20.2	120
17	Accelerating Triple Transport in Zincâ€Air Batteries and Water Electrolysis by Spatially Confining Co Nanoparticles in Breathable Honeycombâ€Like Macroporous Nâ€Đoped Carbon. Small, 2021, 17, e2103517.	10.0	43

#	Article	IF	CITATIONS
19	One-step construction of a transition-metal surface decorated with metal sulfide nanoparticles: A high-efficiency electrocatalyst for hydrogen generation. Journal of Colloid and Interface Science, 2020, 558, 1-8.	9.4	31
20	Hierarchical MoS2/NiCo2S4@C urchin-like hollow microspheres for asymmetric supercapacitors. Chemical Engineering Journal, 2020, 380, 122544.	12.7	143
21	A one-pot "shielding-to-etching―strategy to synthesize amorphous MoS ₂ modified CoS/Co _{0.85} Se heterostructured nanotube arrays for boosted energy-saving H ₂ generation. Nanoscale, 2020, 12, 991-1001.	5.6	33
22	Thickness-dependent carrier separation in Bi2Fe4O9 nanoplates with enhanced photocatalytic water oxidation. Chemical Engineering Journal, 2020, 385, 123929.	12.7	70
23	Hierarchical molybdenum-doped cobaltous hydroxide nanotubes assembled by cross-linked porous nanosheets with efficient electronic modulation toward overall water splitting. Journal of Colloid and Interface Science, 2020, 562, 400-408.	9.4	29
24	Visibleâ€Lightâ€Driven Electrocatalytic Oxygen Evolution Reaction: NiFe ₂ O ₄ /NiFe–Layered Double Hydroxide Zâ€6cheme Heteronanosheet as a Model. Energy Technology, 2020, 8, 2000607.	3.8	6
25	Hierarchical Cu ₂ S@NiCo-LDH double-shelled nanotube arrays with enhanced electrochemical performance for hybrid supercapacitors. Journal of Materials Chemistry A, 2020, 8, 22163-22174.	10.3	159
26	Construction of sugar-gourd-shaped CdS/Co1-xS hollow hetero-nanostructure as an efficient Z-scheme photocatalyst for hydrogen generation. Chemical Engineering Journal, 2020, 400, 125925.	12.7	76
27	An efficient and stable Ni–Fe selenides/nitrogen-doped carbon nanotubes in situ-derived electrocatalyst for oxygen evolution reaction. Journal of Materials Science, 2020, 55, 13927-13937.	3.7	27
28	Copolymerization of 2-(perfluorohexyl)ethyl methacrylate with divinylbenzene to fluorous porous polymeric materials as fluorophilic absorbents. Microporous and Mesoporous Materials, 2020, 305, 110398.	4.4	2
29	Enhanced Photoactivity and Photostability for Visibleâ€Lightâ€Driven Water Oxidation over BiFeO ₃ Porous Nanotubes by Modification of Mo Doping and Carbon Nanocoating. ChemNanoMat, 2020, 6, 1325-1331.	2.8	24
30	Theoretical Evidence on the Confinement Effect of Pt@UiO-66-NH ₂ for Cinnamaldehyde Hydrogenation. Journal of Physical Chemistry C, 2019, 123, 22114-22122.	3.1	28
31	Construction of CoO/Coâ€Cuâ€ S Hierarchical Tubular Heterostructures for Hybrid Supercapacitors. Angewandte Chemie, 2019, 131, 15587-15593.	2.0	80
32	Construction of CoO/Coâ€Cuâ€S Hierarchical Tubular Heterostructures for Hybrid Supercapacitors. Angewandte Chemie - International Edition, 2019, 58, 15441-15447.	13.8	346
33	Ammonia-steam treated FeZSM-5 for direct N2O decomposition. Microporous and Mesoporous Materials, 2019, 290, 109655.	4.4	5
34	Facile in situ fabrication of Co nanoparticles embedded in 3D N-enriched mesoporous carbon foam electrocatalyst with enhanced activity and stability toward oxygen reduction reaction. Journal of Materials Science, 2019, 54, 5412-5423.	3.7	47
35	A facile sequential ion exchange strategy to synthesize CoSe ₂ /FeSe ₂ double-shelled hollow nanocuboids for the highly active and stable oxygen evolution reaction. Nanoscale, 2019, 11, 10738-10745.	5.6	80
36	Facile in-situ growth of Ni2P/Fe2P nanohybrids on Ni foam for highly efficient urea electrolysis. Journal of Colloid and Interface Science, 2019, 541, 279-286.	9.4	113

#	Article	IF	CITATIONS
37	Electronic modulation of composite electrocatalysts derived from layered NiFeMn triple hydroxide nanosheets for boosted overall water splitting. Nanoscale, 2019, 11, 20797-20808.	5.6	30
38	Beyond CoO _x : a versatile amorphous cobalt species as an efficient cocatalyst for visible-light-driven photocatalytic water oxidation. Chemical Communications, 2019, 55, 14050-14053.	4.1	38
39	A new photocatalyst based on Co(CO3)0.5(OH)·0.11H2O/Bi2WO6 nanocomposites for high-efficiency cocatalyst-free O2 evolution. Chemical Engineering Journal, 2019, 359, 924-932.	12.7	59
40	One-Step Solvothermal Formation of Pt Nanoparticles Decorated Pt ²⁺ -Doped α-Fe ₂ O ₃ Nanoplates with Enhanced Photocatalytic O ₂ Evolution. ACS Catalysis, 2019, 9, 1211-1219.	11.2	167
41	Construction of mesoporous Cu-doped Co ₉ S ₈ rectangular nanotube arrays for high energy density all-solid-state asymmetric supercapacitors. Journal of Materials Chemistry A, 2019, 7, 5333-5343.	10.3	150
42	A Roomâ€Temperature Postsynthetic Ligand Exchange Strategy to Construct Mesoporous Feâ€Doped CoP Hollow Triangle Plate Arrays for Efficient Electrocatalytic Water Splitting. Small, 2018, 14, e1704233.	10.0	244
43	Earthâ€Abundant Silicon for Facilitating Water Oxidation over Ironâ€Based Perovskite Electrocatalyst. Advanced Materials Interfaces, 2018, 5, 1701693.	3.7	53
44	Dodecylamineâ€Induced Synthesis of a Nitrogenâ€Doped Carbon Comb for Advanced Lithium–Sulfur Battery Cathodes. Advanced Materials Interfaces, 2018, 5, 1701659.	3.7	21
45	Fabrication of Porous Cu-Doped BiVO ₄ Nanotubes as Efficient Oxygen-Evolving Photocatalysts. ACS Applied Nano Materials, 2018, 1, 2589-2599.	5.0	63
46	Electrospinning preparation of Sn4+-doped BiFeO3 nanofibers as efficient visible-light-driven photocatalyst for O2 evolution. Journal of Alloys and Compounds, 2018, 766, 274-283.	5.5	37
47	Reduced CoNi2S4 nanosheets with enhanced conductivity for high-performance supercapacitors. Electrochimica Acta, 2018, 278, 33-41.	5.2	114
48	Scalable fabrication of ZnxCd1-xS double-shell hollow nanospheres for highly efficient hydrogen production. Applied Catalysis B: Environmental, 2018, 239, 309-316.	20.2	82
49	Construction of hierarchical FeP/Ni ₂ P hollow nanospindles for efficient oxygen evolution. Journal of Materials Chemistry A, 2018, 6, 14103-14111.	10.3	109
50	Facile preparation of ternary Ag2CO3/Ag/PANI composite nanorods with enhanced photoactivity and stability. Journal of Materials Science, 2017, 52, 4521-4531.	3.7	16
51	A facile sacrificial template method to synthesize one-dimensional porous CdO/CdFe ₂ O ₄ hybrid nanoneedles with superior adsorption performance. RSC Advances, 2017, 7, 5093-5100.	3.6	8
52	High-performance non-enzymatic perovskite sensor for hydrogen peroxide and glucose electrochemical detection. Sensors and Actuators B: Chemical, 2017, 244, 482-491.	7.8	82
53	Mixed Conducting Perovskite Materials as Superior Catalysts for Fast Aqueous-Phase Advanced Oxidation: A Mechanistic Study. ACS Catalysis, 2017, 7, 388-397.	11.2	260
54	One-Step Solvothermal Synthesis of Petalous Carbon-Coated Cu ⁺ -Doped CdS Nanocomposites with Enhanced Photocatalytic Hydrogen Production. Langmuir, 2017, 33, 6719-6726.	3.5	67

#	Article	IF	CITATIONS
55	Hierarchical Porous Yolk–Shell Carbon Nanosphere for Highâ€Performance Lithium–Sulfur Batteries. Particle and Particle Systems Characterization, 2017, 34, 1600281.	2.3	34
56	Unusual formation of tetragonal microstructures from nitrogen-doped carbon nanocapsules with cobalt nanocores as a bi-functional oxygen electrocatalyst. Journal of Materials Chemistry A, 2017, 5, 2271-2279.	10.3	80
57	A Perovskite Nanorod as Bifunctional Electrocatalyst for Overall Water Splitting. Advanced Energy Materials, 2017, 7, 1602122.	19.5	369
58	Band-gap engineering of porous BiVO ₄ nanoshuttles by Fe and Mo co-doping for efficient photocatalytic water oxidation. Inorganic Chemistry Frontiers, 2017, 4, 2045-2054.	6.0	59
59	Fructoseâ€Derived Hollow Carbon Nanospheres with Ultrathin and Ordered Mesoporous Shells as Cathodes in Lithium–Sulfur Batteries for Fast Energy Storage. Advanced Sustainable Systems, 2017, 1, 1700081.	5.3	27
60	An extremely active and durable Mo 2 C/graphene-like carbon based electrocatalyst for hydrogen evolution reaction. Materials Today Energy, 2017, 6, 230-237.	4.7	18
61	Facile synthesis of nitrogen-doped carbon nanotubes encapsulating nickel cobalt alloys 3D networks for oxygen evolution reaction in an alkaline solution. Journal of Power Sources, 2017, 338, 26-33.	7.8	105
62	LiNi0.29Co0.33Mn0.38O2 polyhedrons with reduced cation mixing as a high-performance cathode material for Li-ion batteries synthesized via a combined co-precipitation and molten salt heating technique. Journal of Alloys and Compounds, 2017, 691, 206-214.	5.5	35
63	High performance porous iron oxide-carbon nanotube nanocomposite as an anode material for lithium-ion batteries. Electrochimica Acta, 2016, 212, 179-186.	5.2	34
64	Phosphorusâ€Doped Perovskite Oxide as Highly Efficient Water Oxidation Electrocatalyst in Alkaline Solution. Advanced Functional Materials, 2016, 26, 5862-5872.	14.9	271
65	Lithium-Ion Batteries: Mesoporous and Nanostructured TiO2 layer with Ultra-High Loading on Nitrogen-Doped Carbon Foams as Flexible and Free-Standing Electrodes for Lithium-Ion Batteries (Small 48/2016). Small, 2016, 12, 6768-6768.	10.0	0
66	One-pot combustion synthesis of Li3VO4-Li4Ti5O12 nanocomposite as anode material of lithium-ion batteries with improved performance. Electrochimica Acta, 2016, 222, 587-595.	5.2	12
67	Trapping sulfur in hierarchically porous, hollow indented carbon spheres: a high-performance cathode for lithium–sulfur batteries. Journal of Materials Chemistry A, 2016, 4, 9526-9535.	10.3	100
68	Optimal hydrothermal synthesis of hierarchical porous ZnMn 2 O 4 microspheres with more porous core for improved lithium storage performance. Electrochimica Acta, 2016, 207, 58-65.	5.2	24
69	Magnetic Core–Shell Nanostructured Palladium Catalysts for Green Oxidation of Benzyl Alcohol. Catalysis Letters, 2016, 146, 1321-1330.	2.6	16
70	Mesoporous and Nanostructured TiO ₂ layer with Ultraâ€High Loading on Nitrogenâ€Doped Carbon Foams as Flexible and Freeâ€Standing Electrodes for Lithiumâ€Ion Batteries. Small, 2016, 12, 6724-6734.	10.0	79
71	Facile synthesis of porous Bi2O3-BiVO4 p-n heterojunction composite microrods with highly efficient photocatalytic degradation of phenol. Journal of Alloys and Compounds, 2016, 688, 1080-1087.	5.5	60
72	Facile one-pot solvothermal preparation of Mo-doped Bi ₂ WO ₆ biscuit-like microstructures for visible-light-driven photocatalytic water oxidation. Journal of Materials Chemistry A, 2016, 4, 13242-13250.	10.3	88

#	Article	IF	CITATIONS
73	Highly Active Carbon/αâ€MnO ₂ Hybrid Oxygen Reduction Reaction Electrocatalysts. ChemElectroChem, 2016, 3, 1760-1767.	3.4	42
74	Synthesis, Carbonization, and CO ₂ Adsorption Properties of Phloroglucinol–Melamine–Formaldehyde Polymeric Nanofibers. Industrial & Engineering Chemistry Research, 2016, 55, 12667-12674.	3.7	19
75	Surfactant-free self-assembly of reduced graphite oxide-MoO2 nanobelt composites used as electrode for lithium-ion batteries. Electrochimica Acta, 2016, 211, 972-981.	5.2	53
76	Direct Generation of Fine Bi ₂ WO ₆ Nanocrystals on g ₃ N ₄ Nanosheets for Enhanced Photocatalytic Activity. ChemNanoMat, 2016, 2, 732-738.	2.8	25
77	A hierarchical Zn ₂ Mo ₃ O ₈ nanodots–porous carbon composite as a superior anode for lithium-ion batteries. Chemical Communications, 2016, 52, 9402-9405.	4.1	29
78	Facile synthesis of a MoO2–Mo2C–C composite and its application as favorable anode material for lithium-ion batteries. Journal of Power Sources, 2016, 307, 552-560.	7.8	98
79	Process Investigation of a Solid Carbon-Fueled Solid Oxide Fuel Cell Integrated with a CO ₂ -Permeating Membrane and a Sintering-Resistant Reverse Boudouard Reaction Catalyst. Energy & amp; Fuels, 2016, 30, 1841-1848.	5.1	16
80	Improved performance of hierarchical Fe-ZSM-5 in the direct oxidation of benzene to phenol by N2O. Microporous and Mesoporous Materials, 2016, 227, 252-257.	4.4	28
81	Synergetic catalysis of palladium nanoparticles encaged within amine-functionalized UiO-66 in the hydrodeoxygenation of vanillin in water. Green Chemistry, 2016, 18, 2900-2908.	9.0	175
82	Simultaneous formation of silica-protected and N-doped TiO ₂ hollow spheres using organic–inorganic silica as self-removed templates. Journal of Materials Chemistry A, 2015, 3, 2234-2241.	10.3	26
83	Facile Conversion of Commercial Coarse-Type LiCoO ₂ to Nanocomposite-Separated Nanolayer Architectures as a Way for Electrode Performance Enhancement. ACS Applied Materials & Interfaces, 2015, 7, 1787-1794.	8.0	17
84	Polyoxometalates confined in the mesoporous cages of metal–organic framework MIL-100(Fe): Efficient heterogeneous catalysts for esterification and acetalization reactions. Chemical Engineering Journal, 2015, 269, 236-244.	12.7	128
85	A Carbon–Air Battery for High Power Generation. Angewandte Chemie - International Edition, 2015, 54, 3722-3725.	13.8	40
86	Facile synthesis of Z-scheme Ag ₂ CO ₃ /Ag/AgBr ternary heterostructured nanorods with improved photostability and photoactivity. Journal of Materials Chemistry A, 2015, 3, 5474-5481.	10.3	123
87	Synthesis of vis/NIR-driven hybrid photocatalysts by electrostatic assembly of NaYF4:Yb, Tm nanocrystals on g-C3N4 nanosheets. Materials Letters, 2015, 146, 87-90.	2.6	28
88	Carbon-coated Fe ₃ O ₄ microspheres with a porous multideck-cage structure for highly reversible lithium storage. Chemical Communications, 2015, 51, 6921-6924.	4.1	54
89	Palladium nanoparticles incorporated within sulfonic acid-functionalized MIL-101(Cr) for efficient catalytic conversion of vanillin. Journal of Materials Chemistry A, 2015, 3, 17008-17015.	10.3	107
90	Direct coating ZnO nanocrystals onto 1D Fe3O4/C composite microrods as highly efficient and reusable photocatalysts for water treatment. Journal of Alloys and Compounds, 2015, 637, 301-307.	5.5	23

#	Article	IF	CITATIONS
91	Facile fabrication of mesoporous BiOCl/(BiO) ₂ CO ₃ /Bi ₂ O ₃ ternary flower-like heterostructured microspheres with high visible-light-driven photoactivity. Journal of Materials Chemistry A, 2015, 3, 22413-22420.	10.3	37
92	Facile Formation of Mesoporous BiVO ₄ /Ag/AgCl Heterostructured Microspheres with Enhanced Visible-Light Photoactivity. Inorganic Chemistry, 2015, 54, 9033-9039.	4.0	108
93	Facile formation of Ag2WO4/AgX (X=Cl, Br, I) hybrid nanorods with enhanced visible-light-driven photoelectrochemical properties. Materials Research Bulletin, 2015, 61, 315-320.	5.2	48
94	Facile synthesis of MIL-100(Fe) under HF-free conditions and its application in the acetalization of aldehydes with diols. Chemical Engineering Journal, 2015, 259, 183-190.	12.7	237
95	Hydroxylation of Benzene to Phenol by H2O2 over an Inorganic–Organic Dual Modified Heteropolyacid. Chinese Journal of Chemical Engineering, 2014, 22, 1220-1225.	3.5	7
96	Formation of Mesoporous Heterostructured BiVO ₄ /Bi ₂ S ₃ Hollow Discoids with Enhanced Photoactivity. Angewandte Chemie - International Edition, 2014, 53, 5917-5921.	13.8	269
97	Magnetically Responsive Core–Shell Pd/Fe3O4@C Composite Catalysts for the Hydrogenation of Cinnamaldehyde. Catalysis Letters, 2014, 144, 2065-2070.	2.6	13
98	A stepwise loading method to magnetically responsive Pt-Fe3O4/MCNT catalysts for selective hydrogenation of 3-methylcrotonaldehyde. Nanoscale Research Letters, 2014, 9, 2498.	5.7	4
99	Triethylamine-modified Keggin heteropolyacid: a novel phase-transfer catalyst for hydroxylation of benzene with H2O2. Research on Chemical Intermediates, 2014, 40, 1867-1877.	2.7	4
100	Synthesis of sulfonic acid-functionalized MIL-101 for acetalization of aldehydes with diols. Journal of Molecular Catalysis A, 2014, 383-384, 167-171.	4.8	77
101	Facile preparation of 2D sandwich-like CdS nanoparticles/nitrogen-doped reduced graphene oxide hybrid nanosheets with enhanced photoelectrochemical properties. Journal of Materials Chemistry A, 2014, 2, 19815-19821.	10.3	47
102	Self-assembly of LaF ₃ :Yb,Er/Tm nanoplates into colloidal spheres and tailoring their upconversion emissions with fluorescent dyes. Journal of Materials Chemistry C, 2014, 2, 8949-8955.	5.5	14
103	Controllable growth of SnS2/SnO2 heterostructured nanoplates via a hydrothermal-assisted self-hydrolysis process and their visible-light-driven photocatalytic reduction of Cr(vi). RSC Advances, 2014, 4, 29698-29701.	3.6	35
104	Rapid formation of AgnX(X = S, Cl, PO4, C2O4) nanotubes via an acid-etching anion exchange reaction. Nanoscale, 2014, 6, 5612-5615.	5.6	21
105	Synthesis of small yolk–shell Fe3O4@TiO2 nanoparticles with controllable thickness as recyclable photocatalysts. RSC Advances, 2014, 4, 8901.	3.6	42
106	<i>In Situ</i> Transmission Electron Microscopy Observation of Electrochemical Sodiation of Individual Co ₉ S ₈ -Filled Carbon Nanotubes. ACS Nano, 2014, 8, 3620-3627.	14.6	76
107	Directly coat TiO ₂ on hydrophobic NaYF ₄ :Yb,Tm nanoplates and regulate their photocatalytic activities with the core size. Journal of Materials Chemistry A, 2014, 2, 13486-13491.	10.3	60
108	Utilizing the Gate-Opening Mechanism in ZIF-7 for Adsorption Discrimination between N ₂ O and CO ₂ . Journal of Physical Chemistry C, 2014, 118, 17831-17837.	3.1	51

#	Article	IF	CITATIONS
109	Enhanced Sulfur Tolerance of Nickel-Based Anodes for Oxygen-Ion Conducting Solid Oxide Fuel Cells by Incorporating a Secondary Water Storing Phase. Environmental Science & Technology, 2014, 48, 12427-12434.	10.0	23
110	Catalytic hydrogenation of 2,3,5-trimethylbenzoquinone over Pd nanoparticles confined in the cages of MIL-101(Cr). Chemical Engineering Journal, 2014, 239, 33-41.	12.7	59
111	In Situ Transmission Electron Microscopy Observation of Electrochemical Behavior of CoS ₂ in Lithium-Ion Battery. ACS Applied Materials & Interfaces, 2014, 6, 3016-3022.	8.0	129
112	Controllable one-pot synthesis of various one-dimensional Bi2S3 nanostructures and their enhanced visible-light-driven photocatalytic reduction of Cr(VI). Journal of Alloys and Compounds, 2014, 611, 335-340.	5.5	43
113	Atomâ€Economic Synthesis of Optically Active Warfarin Anticoagulant over a Chiral MOF Organocatalyst. Advanced Synthesis and Catalysis, 2013, 355, 2538-2543.	4.3	33
114	Highly stable chromium(III) terephthalate metal organic framework (MIL-101) encapsulated 12-tungstophosphoric heteropolyacid as a water-tolerant solid catalyst for hydrolysis and esterification. Reaction Kinetics, Mechanisms and Catalysis, 2013, 109, 77-89.	1.7	35
115	Polyoxometalate-Based Amphiphilic Catalysts for Selective Oxidation of Benzyl Alcohol with Hydrogen Peroxide under Organic Solvent-Free Conditions. Industrial & Engineering Chemistry Research, 2013, 52, 10095-10104.	3.7	46
116	Comparison study on strategies to prepare nanocrystalline Li2ZrO3-based absorbents for CO2 capture at high temperatures. Frontiers of Chemical Science and Engineering, 2013, 7, 297-302.	4.4	20
117	<i>In Situ</i> Transmission Electron Microscopy Investigation of the Electrochemical Lithiation–Delithiation of Individual Co ₉ S ₈ /Co-Filled Carbon Nanotubes. ACS Nano, 2013, 7, 11379-11387.	14.6	70
118	Facile Clâ^'-mediated hydrothermal synthesis of large-scale Ag nanowires from AgCl hydrosol. CrystEngComm, 2013, 15, 2598.	2.6	30
119	A localized crystallization to hierarchical ZSM-5 microspheres aided by silane coupling agent. Journal of Colloid and Interface Science, 2013, 394, 604-610.	9.4	17
120	Facile synthesis of porous bifunctional Fe3O4@Y2O3:Ln nanocomposites using carbonized ferrocene as templates. RSC Advances, 2013, 3, 25970.	3.6	4
121	Microwave-assisted deposition of metal sulfide/oxide nanocrystals onto a 3D hierarchical flower-like TiO2 nanostructure with improved photocatalytic activity. Journal of Materials Chemistry A, 2013, 1, 8101.	10.3	64
122	A heterostructured Ag@In2S3 composite with enhanced lithium storage capacity. Journal of Materials Chemistry A, 2013, 1, 5208.	10.3	13
123	Facile one-pot synthesis of uniform TiO2–Ag hybrid hollow spheres with enhanced photocatalytic activity. Dalton Transactions, 2013, 42, 1122-1128.	3.3	114
124	Sulfonic acid-functionalized MIL-101 as a highly recyclable catalyst for esterification. Catalysis Science and Technology, 2013, 3, 2044.	4.1	92
125	Facile synthesis of uniform FeZSM-5 crystals with controlled size and their application to N2O decomposition. Microporous and Mesoporous Materials, 2013, 167, 38-43.	4.4	14
126	Synthesis of MIL-100(Fe) at Low Temperature and Atmospheric Pressure. Journal of Chemistry, 2013, 2013, 1-4.	1.9	24

#	Article	IF	CITATIONS
127	Li ₂ ZrO ₃ Nanoparticles as Absorbent for in-Situ Removal of CO ₂ in Water-Gas Shift Reaction to Enhance H ₂ Production. Chinese Journal of Catalysis, 2013, 33, 1572-1577.	14.0	1
128	Facile Low-Temperature Synthesis of Carbon Nanotube/ Nanohybrids with Enhanced Visible-Light-Driven Photocatalytic Activity. International Journal of Photoenergy, 2012, 2012, 1-6.	2.5	13
129	Innenrücktitelbild: Microwave-Assisted Synthesis of Porous Ag2S-Ag Hybrid Nanotubes with High Visible-Light Photocatalytic Activity (Angew. Chem. 46/2012). Angewandte Chemie, 2012, 124, 11807-11807.	2.0	0
130	Microwaveâ€Assisted Synthesis of Porous Ag ₂ S–Ag Hybrid Nanotubes with High Visible‣ight Photocatalytic Activity. Angewandte Chemie - International Edition, 2012, 51, 11501-11504.	13.8	215
131	Synthesis and characterization of large, pure mordenite crystals. Journal of Porous Materials, 2012, 19, 847-852.	2.6	9
132	One-pot synthesis of nitroalkenes via the Henry reaction over amino-functionalized MIL-101 catalysts. Catalysis Communications, 2012, 29, 101-104.	3.3	32
133	Phase transition of manganese (oxyhydr)oxides nanofibers and their applications to lithium ion batteries and separation membranes. CrystEngComm, 2012, 14, 3142.	2.6	13
134	Selective adsorption of CO2 on amino-functionalized silica spheres with centrosymmetric radial mesopores and high amino loading. Adsorption, 2012, 18, 423-430.	3.0	10
135	Facile and rapid synthesis of RGO–In2S3 composites with enhanced cyclability and high capacity for lithium storage. Nanoscale, 2012, 4, 7354.	5.6	53
136	Ultrathin SnO ₂ Nanosheets: Oriented Attachment Mechanism, Nonstoichiometric Defects, and Enhanced Lithium-Ion Battery Performances. Journal of Physical Chemistry C, 2012, 116, 4000-4011.	3.1	325
137	A Facile Starchâ€Assisted Sol–Gel Method to Synthesize Kâ€Doped <scp><scp>Li</scp></scp> 2 <scp><scp>ZrO</scp>3 Sorbents with Excellent <scp><scp>CO</scp></scp>2 Capture Properties. Journal of the American Ceramic Society, 2012, 95, 1544-1548.</scp>	3.8	25
138	Adsorption of Pb2+ and Cu2+ on anionic surfactant-templated amino-functionalized mesoporous silicas. Chemical Engineering Journal, 2012, 189-190, 160-167.	12.7	65
139	Direct oxidation of benzene to phenol by N2O over meso-Fe-ZSM-5 catalysts obtained via alkaline post-treatment. Catalysis Science and Technology, 2011, 1, 1250.	4.1	41
140	Large-scale synthesis of In2S3 nanosheets and their rechargeable lithium-ion battery. Journal of Materials Chemistry, 2011, 21, 17063.	6.7	59
141	A citrate sol–gel method to synthesize Li2ZrO3 nanocrystals with improved CO2 capture properties. Journal of Materials Chemistry, 2011, 21, 3838.	6.7	73
142	One-Pot Synthesis and CO ₂ Adsorption Properties of Ordered Mesoporous SBA-15 Materials Functionalized with APTMS. Journal of Physical Chemistry C, 2011, 115, 12873-12882.	3.1	63
143	Salt-induced synthesis of sheet-like SBA-15 under neutral conditions. Journal of Porous Materials, 2011, 18, 553-556.	2.6	0
144	Deactivation of Pd/C catalysts in the hydrodechlorination of the chlorofluorocarbons CFC-115 and CFC-12. Catalysis Today, 2011, 175, 615-618.	4.4	15

#	Article	IF	CITATIONS
145	Citrate route to prepare K-doped Li2ZrO3 sorbents with excellent CO2 capture properties. Chemical Engineering Journal, 2011, 174, 231-235.	12.7	54
146	Synthesis and CO2 adsorption property of amino-functionalized silica nanospheres with centrosymmetric radial mesopores. Microporous and Mesoporous Materials, 2010, 132, 552-558.	4.4	38
147	Comparison Study on the Adsorption of CFC-115 and HFC-125 on Activated Carbon and Silicalite-1. Industrial & Engineering Chemistry Research, 2010, 49, 10009-10015.	3.7	17
148	A simple H2O2-assisted route to hollow TiO2 structures with different crystal structures and morphologies. Materials Research Bulletin, 2009, 44, 999-1002.	5.2	22
149	Adsorption of Nitrous Oxide on Activated Carbons. Journal of Chemical & Engineering Data, 2009, 54, 3079-3081.	1.9	25
150	Synthesis of bimodal mesoporous molecular sieves under mild conditions with salts as mineralization agents. Microporous and Mesoporous Materials, 2008, 116, 339-343.	4.4	7
151	Reactant-selective oxidation over composite zeolite-4A coated Pt/Î ³ -Al2O3 particles. Studies in Surface Science and Catalysis, 2007, 170, 1313-1318.	1.5	1
152	Fabrication of zeolite-4A membranes on a catalyst particle level. Chemical Communications, 2006, , 2911.	4.1	11